ground water

Estimation of Hydraulic Conductivity in an Alluvial System Using Temperatures

by Grace W. Su[1], James Jasperse[2], Donald Seymour[2], and Jim Constantz[3]

Abstract

Well water temperatures are often collected simultaneously with water levels; however, temperature data are generally considered only as a water quality parameter and are not utilized as an environmental tracer. In this paper, water levels and seasonal temperatures are used to estimate hydraulic conductivities in a stream-aquifer system. To demonstrate this method, temperatures and water levels are analyzed from six observation wells along an example study site, the Russian River in Sonoma County, California. The range in seasonal ground water temperatures in these wells varied from < 0.2°C in two wells to ~8°C in the other four wells from June to October 2000. The temperature probes in the six wells are located at depths between 3.5 and 7.1 m relative to the river channel. Hydraulic conductivities are estimated by matching simulated ground water temperatures to the observed ground water temperatures. An anisotropy of 5 (horizontal to vertical hydraulic conductivity) generally gives the best fit to the observed temperatures. Estimated conductivities vary over an order of magnitude in the six locations analyzed. In some locations, a change in the observed temperature profile occurred during the study, most likely due to deposition of fine-grained sediment and organic matter plugging the streambed. A reasonable fit to this change in the temperature profile is obtained by decreasing the hydraulic conductivity in the simulations. This study demonstrates that seasonal ground water temperatures monitored in observation wells provide an effective means of estimating hydraulic conductivities in alluvial aquifers.

Introduction

Quantifying surface water/ground water exchanges has become an important component of water resources management because of the increase in the conjunctive use of water. Reducing uncertainty in models used to select an optimal operation management alternative requires proper identification of the spatial and temporal variations in physical parameters such as the hydraulic conductivity of the streambed and aquifer. Recently, heat as a tracer has been demonstrated to be a robust method for quantifying surface water/ground water exchanges in a range of environments—from perennial streams in humid regions (Lapham 1989; Silliman and Booth 1993) to ephemeral channels in arid locations (Constantz and Thomas 1996; Constantz et al. 2001; Constantz et al. 2002; Stonestrom and Constantz 2003). In these studies, diurnal temperature profiles were measured and analyzed to quantify streambed fluxes and hydraulic conductivities. Diurnal temperature variations typically occur over a shallow depth in the range of 0.2 to 2 m (Constantz et al. 2003). At greater depths, weekly and seasonal temperature variations may be observed where the temperatures vary over several days or months rather than during a day. These temperature profiles provide estimates of conductivities over a larger spatial and temporal scale (Lapham 1989; Bartolino and Niswonger 1999; Mihevc et al. 2001) compared to those obtained from diurnal temperature profiles.

In addition to quantifying surface water/ground water exchanges, temperature has also been used as a tool for estimating ground water fluxes and recharge rates in aquifers and wetlands. Steady-state temperature-depth profiles have been used to estimate these parameters in aquifers and in wetland systems (Boyle and Saleem 1979; Hunt et al. 1996;

[1]Corresponding author: Lawrence Berkeley National Laboratory, Earth Sciences Division, Berkeley, CA 94720; (510) 495–2338; gwsu@lbl.gov
[2]Sonoma County Water Agency, Santa Rosa, CA 95406
[3]U.S. Geological Survey, Menlo Park, CA 94025
Received June 2003, accepted February 2004.
Published in 2004 by the National Ground Water Association.

Taniguchi et al. 1999; Fergerson et al. 2003), and seasonal ground water temperature profiles have been used to determine ground water fluxes in shallow aquifers (Taniguchi 1993). Ground water temperature data have also been used in conjunction with water level data to estimate hydraulic conductivities in a deep aquifer system (Woodbury and Smith 1988) and in a wetland system (Bravo et al. 2002).

Ground water temperatures and water levels are frequently monitored in observation wells near streams, but temperature data used in conjunction with water level data have not been previously utilized to estimate hydraulic conductivities in a stream-aquifer system. In addition, temperature data from observation wells are generally considered a water quality parameter and are not used as an environmental tracer to characterize hydraulic parameters. Although Bravo et al. (2002) demonstrated that water level and temperature data can be used to constrain hydraulic conductivity estimates, their simulations were conducted using a steady ground water flow and transient heat transport model over a time period when the water level data were constant. In this study, a transient ground water flow and transient heat transport model is used that incorporates the measured variability in water levels. Temperature and water level data are also used in this study to estimate the temporal changes in conductivity.

The objective of this study is to demonstrate that seasonal ground water temperature patterns combined with well water levels can be used to estimate the spatial and temporal variations of hydraulic conductivities in a stream-aquifer system. The Russian River in Sonoma County, California, was selected as an example study site to demonstrate this proof of concept. Temperature and water level data collected from six observation wells between June and October 2000 along the Russian River are analyzed. Two-dimensional ground water flow and heat transport simulations of the region from the river to each observation well are conducted, based on the measured field data. Estimates of hydraulic conductivities are obtained by fitting simulated ground water temperatures to the observed temperatures in the aquifer. The effects of formation anisotropy, layering near the streambed, river stage level, and ground water level on the temperature profiles are also investigated in the simulations.

Russian River, Sonoma County, California

The Russian River is located in northern California, originating in central Mendocino County and flowing into the Pacific Ocean in western Sonoma County. The main channel of the Russian River is ~177 km long and flows southward from its headwaters until Mirabel Park, where the flow direction changes to predominantly westward (Figure 1).

The Russian River provides a major source of municipal water supply for Mendocino, Sonoma, and Marin counties. For example, the Sonoma County Water Agency (SCWA) operates several collector wells along the Russian River with a maximum production capacity of 3.2×10^5 m^3/d that utilize natural filtration processes to provide water supply for more than a half million people in Sonoma and Marin counties. The Russian River is underlain primarily by alluvium and river channel deposits, which consist mainly of unconsolidated sands and gravels, interbedded with thin layers of silt and clay. For the area pertaining to this study, the alluvial aquifer is bounded by metamorphic bedrock (e.g., Franciscan Formation) and is considered impermeable relative to the alluvial materials (California Department of Water Resources 1983).

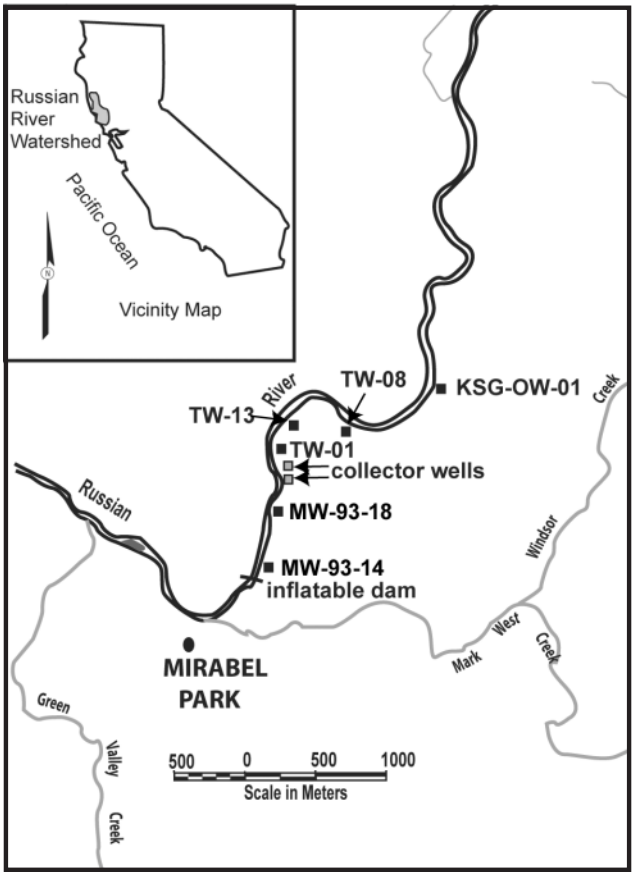

Figure 1. Location of the Russian River in Sonoma County, California, and locations of six observation wells where water levels and ground water temperatures are analyzed.

To enhance water production capacity, the SCWA raises an inflatable dam, typically from the spring through fall seasons, to increase the river stage and passively recharge the alluvial aquifer. In addition, the elevated stage permits diversion of river water to a series of recharge ponds located near the dam along the river. Operation of the inflatable dam creates a backwater that produces lower velocities and higher temperatures in the river that extends ~3200 m upstream of the dam. This low-energy environment promotes the formation of a layer of fine-grained, biologically active material along the bottom of the river, which reduces the conductance of the riverbed.

Field Data

The locations of the six observation wells along the Russian River where water levels and ground water temperatures were recorded and analyzed in this study are shown in Figure 1. The observation wells were constructed of 5.1 cm diameter PVC well casing and a natural filter pack was used. Minitroll vented pressure transducer/temperature probes (In-Situ Inc., Laramie, Wyoming) were installed

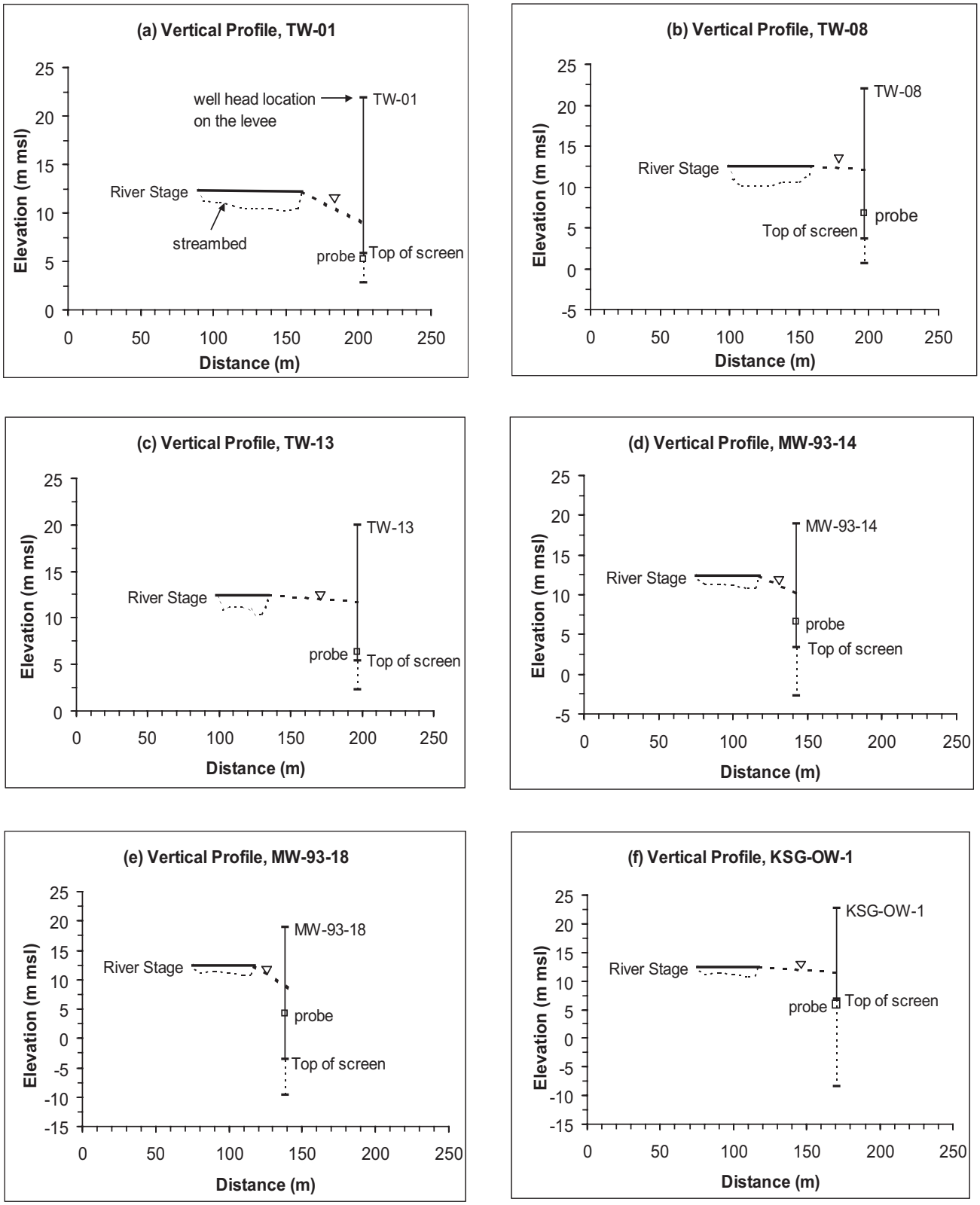

Figure 2. Vertical cross sections of six observation wells showing average water level, river stage, streambed, and location of temperature and pressure probe.

inside the well casing and collected pressure head and temperature data every hour. Vented pressure transducers allowed for automatic compensation of barometric pressure changes. The probes have a temperature accuracy of ± 0.25°C and a pressure accuracy of ± 0.05 m. The location of the probes inside the well casing was determined by the length of cable used to suspend them inside the well casing, which ranged from 15 to 20 m. As a result, the probes were not always located within the screened interval of the six observation wells. We assumed that the temperatures inside the well casing were representative of the surrounding ground water temperatures. Constantz et al. (2002)

Table 1
Measured Distances and Hydraulic Parameters from the Vertical Profiles

Well I.D.	River Stage (m msl)	River Depth (m)	Well Water Level (m msl)	Probe Depth (m Below River Channel)	Horizontal Distance (m from River Bank to Well)	Gradient, *i* (m/m)	Direction
TW-01	12.4	1.9	8.0 ± 0.5	5.8	43	0.010	Toward well
TW-08	12.4	2.0	11.2 ± 0.1	3.5	38	0.037	Toward well
TW-13	12.4	1.5	10.7 ± 0.1	4.5	62	0.027	Toward well
MW-93-14	12.4	1.2	9.8 ± 0.4	4.7	25	0.10	Toward well
MW-93-18	12.4	1.2	8.0 ± 0.9	7.1	21	0.21	Toward well
KSG-OW-01	12.4	1.2	11.5 ± 0.05	5.2	53	0.017	Toward well

compared temperatures measured inside and outside of a PVC piezometer and demonstrated that the temperature difference was minimal.

Well Water Levels and Vertical Cross Sections

Average water levels measured in the six wells between June 16 and October 27, 2000, are shown in the vertical cross sections in Figure 2 and are summarized in Table 1. Table 1 also summarizes the river stage, river depth, horizontal distance from the river bank to the wells, the vertical depth of the temperature probe relative to the river channel, the horizontal hydraulic gradient calculated from the measured river stage and the well water level, and the direction of flow.

The cross sections at each location were extrapolated from annual surveys of the river depth and stage taken along the middle reaches of the Russian River in May 2000. These surveys were conducted over a 5 d period. Although the stage levels had some temporal fluctuations, the average stage level should have remained nearly constant during the study period since these wells were within the backwaters of the inflatable dam. Temporal stage data during the study period were not available for the study site; therefore, an average stage of 12.4 m above mean sea level, which was based on the vertical cross sections, was used at all six well locations. The location closest to the study site where the stage was measured during the study period was Healdsburg, which is located ~6000 m upstream from well KSG-OW-01. The average stage level decreased by only 0.2 m from June to October 2000; therefore, we assumed that 0.2 m was the maximum average stage change near the study site because the stage was more variable in Healdsburg since it was a considerable distance away from the backwaters of the dam. The relative direction of flow at the six locations was determined by the average well water levels and the river stage. In all cases, the flow was from the river to the underlying aquifer, indicating a losing stream.

The measured water level profiles in the six wells are shown in Figure 3. The water levels in TW-01 and MW-93-18 show the most variability over time due to their close proximity to the pumping wells. Less variability in the ground water level is observed in wells TW-08 and MW-93-14, and a nearly constant water level is observed in the two wells farthest away from the pumping wells, KSG-OW-01 and TW-08. The increase in the water level in all six wells that occurred around the middle of January 2001 was due to a large storm event. The inflatable dam was lowered immediately before the storm occurred, and the effect of lowering the dam was evident by the decrease in the well water level after the storm had passed. The increase in the water level ~2 weeks after the dam was lowered was the result of a second storm that occurred in that region.

Stream and Ground Water Temperature Profiles

The stream and the ground water temperature profiles for the six wells are shown in Figure 4. The stream temperatures in the summer average ~21° to 22°C and then decrease during the fall. The ground water temperature profiles vary from a nearly constant temperature in wells TW-08 and KSG-OW-01 to a distinct seasonal pattern of ~8°C in the other four wells. The nearly constant temperature is a result of reduced heat exchange with the stream compared to the other wells, which generally implies less advective heat transport as a result of reduced water fluxes. For example, a low flux vs. a higher flux case can be compared by examining wells TW-08 and TW-13, respectively. The two observation wells have similar horizontal hydraulic gradients, but the observed temperature range is significantly greater for TW-13. Since the thermal conductivity and heat capacity are similar for saturated sands, this large difference in temperature profiles is the result of advective heat transport due to variable water fluxes. The nearly isothermal patterns in TW-08 and KSG-OW-01 indicate the lack of advective heat transport due to low ground water fluxes near the observation point.

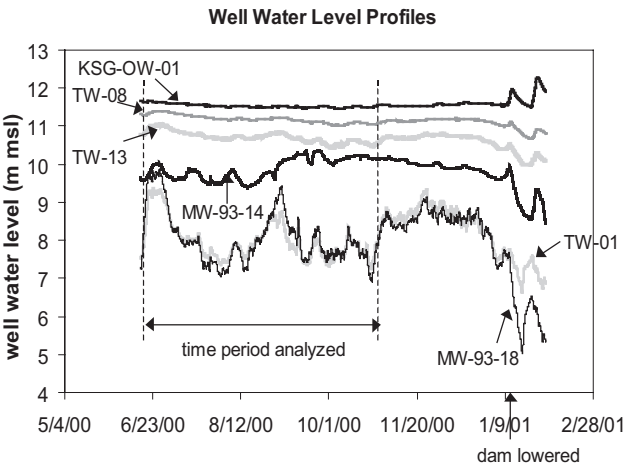

Figure 3. Observed water levels in the six observation wells.

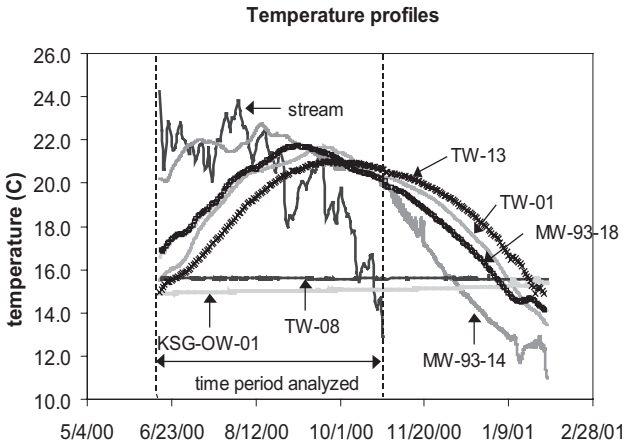

Figure 4. Observed stream temperatures and ground water temperature profiles in the six observation wells. Stream temperatures were recorded only until October 27, 2000.

Numerical Simulations

Two-dimensional simulations of ground water flow and heat transport in a near-stream environment were conducted in this study using VS2DHI (Hsieh et al. 2000), a graphical software package based on VS2DH (Healy and Ronan 1996). VS2DH has been successfully used to describe heat transport in variably saturated material at several sites near streams (Ronan et al. 1998; Constantz et al. 2002). In this study, measured well water levels, stream stage, and stream temperatures were used in the simulations; estimates of the hydraulic conductivities were obtained by fitting simulated ground water temperatures to the observed temperatures from the six observation wells along the Russian River. The unsaturated zone was also included in the simulations because changes in the ground temperature may have an impact on the ground water temperatures in a relatively shallow system.

Governing Equations

VS2DHI simulates heat transport and ground water flow through variably saturated porous media. Heat transport through variably saturated material is described by the advective-dispersive equation

$$\frac{\partial[\theta C_w+(1-\phi)C_s]T}{\partial t}=\nabla\times K_t(\theta)\nabla T+\nabla\times\theta C_w D_h\nabla T-\nabla\times\theta C_w T q+QC_w T \quad (1)$$

where θ is the volumetric fraction of the water content, ϕ is the sediment porosity, K_t is the thermal conductivity of the bulk streambed sediments, D_h is the thermomechanical dispersion tensor, q is the water flux, and Q is the rate of fluid source. C_s and C_w are the specific heat capacities of the water and sediment, respectively. The left side of Equation 1 represents the change in stored energy over time in the pore and solid volume. The first term on the right side describes energy transport by heat conduction, the second term accounts for thermomechanical dispersion, the third term represents advective heat transport, and the final term represents heat sinks or sources to mass movement into or out of the volume. The thermomechanical dispersion tensor is defined as

$$D_h=\alpha_t|v|\delta_{i,j}+\frac{(\alpha_l-\alpha_t)v_i v_j}{|v|} \quad (2)$$

where α_l and α_t are the longitudinal and transverse dispersivities, respectively, $\delta_{i,j}$ is the Kronecker delta function, and v_i, v_j are the ith and jth component of the velocity vector, respectively.

For Equation 1, the water velocity within variably saturated sediments is determined by Richards' equation:

$$C(\psi)\frac{\partial h}{\partial t}=\nabla[K(\psi)\times\nabla h] \quad (3)$$

where $C(\psi)$ is the specific moisture capacity, which is the slope of the retention curve, ψ is the water pressure head, h is the total head, t is time, and K is the hydraulic conductivity. In VS2DH, the dependency of hydraulic conductivity with temperature due to viscosity changes is accounted for, using an empirical formula developed by Kipp (1987).

Simulation Domain

A cross section of the domain used in the numerical simulations is shown in Figure 5. Half of the river channel was simulated with no-flow boundaries on the left and right edges of the domain. A no-flow boundary on the left side was chosen as a symmetry boundary in the middle of the river. A no-flow boundary on the right side was chosen to represent the approximate location of the bedrock contact. The stage levels along the river channel were modeled as a constant head over the duration of the simulations, using the stage from the vertical cross sections (Figure 2). A no-flow boundary condition was used along the ground surface because the period of investigation (June 16 to October 27, 2000) was during the dry season when little or no precipitation occurred. The total head values along the bottom of the domain were varied daily to reproduce the measured water levels at the observation wells. A uniform grid was used in the simulation domain, with each grid element having a 3 m width and 1 m height. The difference in the

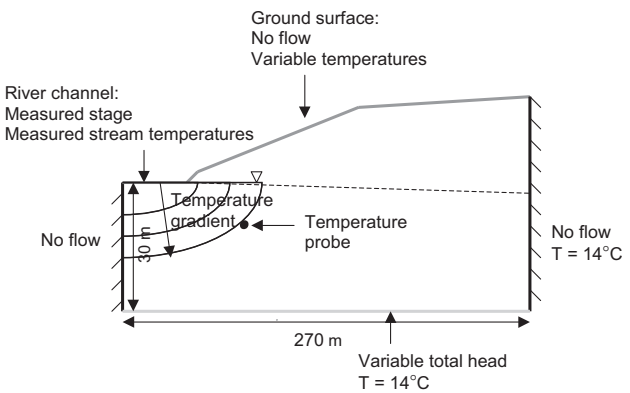

Figure 5. Schematic of simulation domain using VS2DHI.

simulated temperatures using a grid half this size was only 5%. One single domain was used for all six locations since the boundaries of aquifer for all the sites were similar, each of them having a width of ~270 m and a depth below the river streambed of 30 m (the approximate depth of the confining layer).

The measured average daily stream temperatures between June 16 and October 27 were used as the temperature boundary conditions along the river channel. These temperatures were also used to specify the boundary condition representing the ground surface temperatures along the top of the domain. The daily mean ground temperatures were generally close to that of the river water even though the daily range in temperatures at the ground surface was greater than in the stream. The stream and the ground water temperatures observed at the well on June 16 were used to estimate the initial temperature gradient from the stream to the well since stream temperatures measured before June 16 were not available. A schematic of this initial temperature gradient is shown in Figure 5. The uncertainty in the initial temperature profile affected only the simulation results during the initial 1 to 2 weeks. The model was considered accurate once the initial temperature profile was replaced by the simulated ground water temperatures at the location of the temperature probe, which occurred in ~1 to 2 weeks. VS2DHI has a postprocessor that displays the simulation output at each time step; therefore, the output was monitored over time to determine when the simulated temperatures replaced the initial temperatures. The ground water temperature in the remainder of the simulation domain was initially set to 14°C, representative of the regional ground water temperature. Temperatures along the bottom and right side of the domain were held constant at 14°C throughout the simulation. These boundaries were located far enough away from the wells such that they had a < 10% effect on the simulated temperatures at the observation wells.

Transient flow and heat transport simulations were conducted over the study period. The initial time step for each recharge period was 0.5 h, where a recharge period was defined as a time span during which boundary conditions and stresses remained unchanged. For this study, a time span of 1 d was used for each recharge period, resulting in a total of 134 recharge periods. Adaptive time steps with a maximum time step of 3 h were used.

The streambed sediments consisting of interlaced gravels and coarse and fine sands were represented by a homogeneous sand layer in our simulations. Therefore, the estimates of hydraulic conductivities obtained from these simulations were effective values due to the heterogeneity. Simulations were run under isotropic conditions and with anisotropy (horizontal to vertical hydraulic conductivity, K_h/K_v) values of 2 and 5. The goal in changing the anisotropy ratio in the simulations was to determine the physical conditions necessary to make the results more representative of the actual conditions at the sites. This ratio was not changed to finesse out small differences in K. Typically, anisotropy occurs in fluvial environments as textural layering spreads laterally outward from the active channel during the course of sediment deposition that formed the alluvial basin.

Table 2
Summary of Properties Used in VS2DHI Simulations

Property	Value
Porosity (ϕ)	0.37
Heat capacity of dry solids (C_s)	2.18×10^6 J/(m^3 °C)
Heat capacity of water (C_w)	4.18×10^6 J/(m^3 °C)
Thermal conductivity (K_t)	1.0 W/m^3 °C)
Longitudinal thermal dispersivity (α_l)	0.5 m
Transverse thermal dispersivity (α_t)	0.05 m
Anisotropy ratio, K_h/K_v (horizontal to vertical)	1, 2, 5

Table 2 summarizes the soil properties and the heat constants used in the simulations. A porosity of 0.37 was chosen as representative of a medium sand. The heat capacities and thermal conductivity values were based on literature values for sand (Healy and Ronan 1996). The thermal dispersivity value is usually close to zero for small spatial scales, but heterogeneities at greater scales can cause dispersivities to become significant. Longitudinal thermal dispersivity estimated in several field studies ranged from 0 to 3 m (de Marsily 1986). A longitudinal thermal dispersivity of 0.5 m was selected in the present study. A comparison of simulated temperature profiles using longitudinal thermal dispersivities of 0.01 and 0.5 m demonstrated that a superior fit to the observed temperatures was obtained when a dispersivity of 0.5 m was used. The horizontal scale in this study was equal to the 3 m horizontal grid spacing. In a study conducted along the Santa Clara River in southern California (Constantz et al. 2003), a smaller scale (< 1 m) was simulated, and a thermal dispersivity of 0.01 m gave a better fit to the observed temperature profiles compared to a dispersivity of 0.5 m. The larger dispersivity value accounted for sediment heterogeneity. Since the transverse thermal dispersivity is typically ~1/10 of the longitudinal one (de Marsily 1986), a value of 0.05 m was used in our simulations.

Results and Discussion

Simulated Temperature Profiles

Hydraulic conductivities in the six locations were estimated by matching simulated temperatures to the observed temperature data. Different values for the hydraulic conductivity, K, were used in the simulations, and the K value that resulted in the smallest difference between the simulated and observed temperatures for the time period analyzed was considered the best estimate of K. VS2DHI is not currently set up for automated calibration; therefore, a manual calibration was performed. As mentioned earlier, VS2DHI accounts for the change in K with temperature. The K values presented have been normalized to a temperature of 20°C. The simulated results at the different anisotropies (K_h/K_v = 1, 2, 5) in wells TW-13 and MW-93-18 are shown in Figures 6 and 7, respectively. In well TW-13, the best fit K decreases as the anisotropy increases, while the opposite occurs in well MW-93-18, where the best fit K increases as the anisotropy increases. The reason for the different trends in the best fit K as the anisotropy

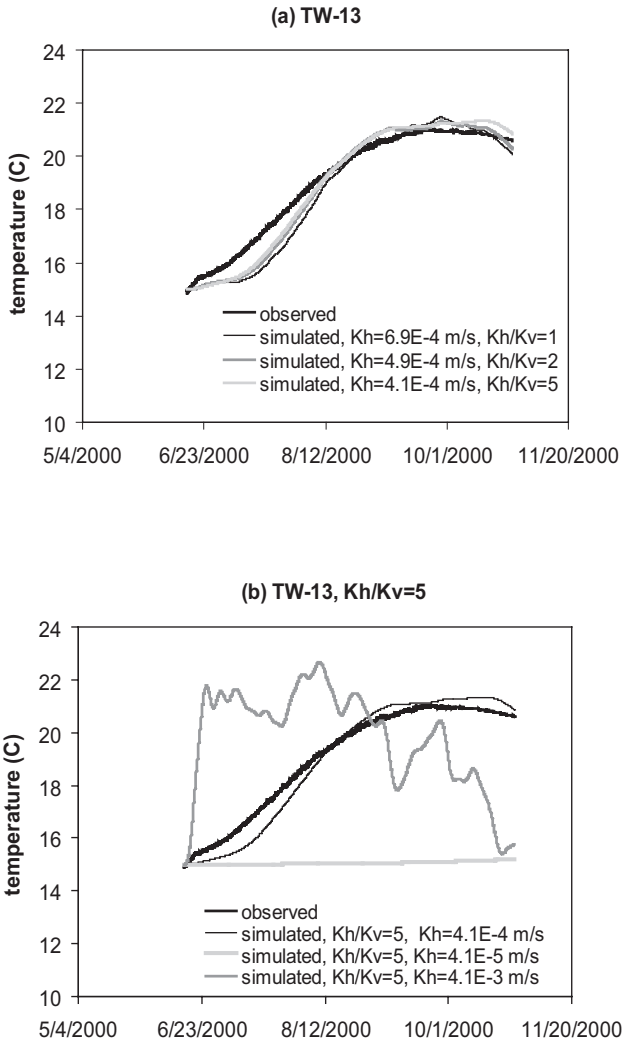

Figure 6. (a) Best-fit simulated temperature profiles for different anisotropy values for well TW-13. (b) Sensitivity of the simulated temperature profiles to large and small *K* values.

changes is discussed in the next section. Visual inspection of the MW-93-18 simulated results indicates that a better fit to the observed temperatures occurs as the anisotropy increases. The fit of the simulated temperature profiles to the observed ones for TW-13 at the different anisotropy values is nearly the same. The sensitivity of the simulated temperature profile in well TW-13 to hydraulic conductivities an order of magnitude larger and smaller than the best fit value ($K = 4.1 \times 10^{-4}$ m/s) is shown in Figure 6b. A large hydraulic conductivity results in a temperature profile that follows the measured stream temperature, while a small *K* results in a nearly constant temperature profile.

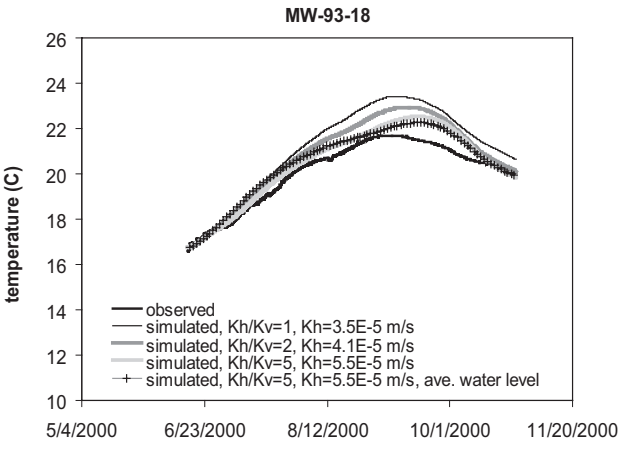

Figure 7. Best-fit simulated temperature profiles for different anisotropy values for well MW-93-18.

The simulated results for well TW-01 are shown in Figure 8a. A good fit between the simulated and the measured temperature profiles is obtained at the different anisotropy values before August, but the fit becomes worse after August. The simulated results oscillate more than the observed temperatures at later times, indicating that a lower conductivity is needed for a better fit. Using a lower conductivity after August results in a much better match to the observed data, as shown in Figure 8b for $K_h/K_v = 5$. The streambed conductivity likely decreases over the summer due to the use of the inflatable dam, which increases the deposition of fine-grained sediment and organic matter that, in turn, plugs the streambed.

The results for well MW-93-14 are shown in Figure 9a. Visual comparison of the simulated results indicates that the best fit to the observed temperatures occurs at an anisotropy of 5 before mid-August. After mid-August, the simulated temperature profile at an anisotropy of 5 is much lower and oscillates more than the observed data. A hydraulic conductivity more than 35% less than the best fit value before mid-August (1.9×10^{-4} m/s) is necessary to obtain a good fit to the measured profile after mid-August for $K_h/K_v = 5$ (Figure 9b). Well 93-14 is located just behind the inflatable dam, so the decrease in *K* is probably due to the accumulation of fine-grained sediments and organic matter behind the inflatable dam. Ground water temperatures and the effective hydraulic conductivity are sensitive to the changes in the hydraulic conductivity along the streambed.

The temperature profiles recorded in wells TW-08 and KSG-OW-01 are nearly constant over time. The maximum *K* values corresponding to where the predicted temperature profiles are no longer constant in these wells are shown in Figures 10a and 10b. Any value of *K* less than the maximum value results in a simulated temperature profile that is constant. The maximum *K* values for well TW-08 are nearly the same as the anisotropy changes, but the *K* values decrease with increasing anisotropy in well KSG-OW-01. Although a maximum *K* value can be obtained when the temperature profile is nearly constant, a seasonal temperature variation of 0.5°C or more would be necessary for estimating *K*. The marked seasonal temperature variation observed in the four other wells was probably due to their proximity to the pumping wells.

The estimated hydraulic conductivities obtained from the temperature profiles recorded in the six observation wells are summarized in Table 3. The hydraulic conductivities vary over one order of magnitude over these six locations, from 5.5×10^{-5} m/s to 4.1×10^{-4} m/s. The *K* values estimated in our study are in the range for a medium to coarse sand, which is typical for alluvium. The estimated *K* values are an arithmetic average of the area between the stream and the observation well. These conductivities were found to be consistent with available geological log data for wells TW-01, TW-08, TW-13, and KSG-OW-01. Geological logs were not available for the remaining wells. The

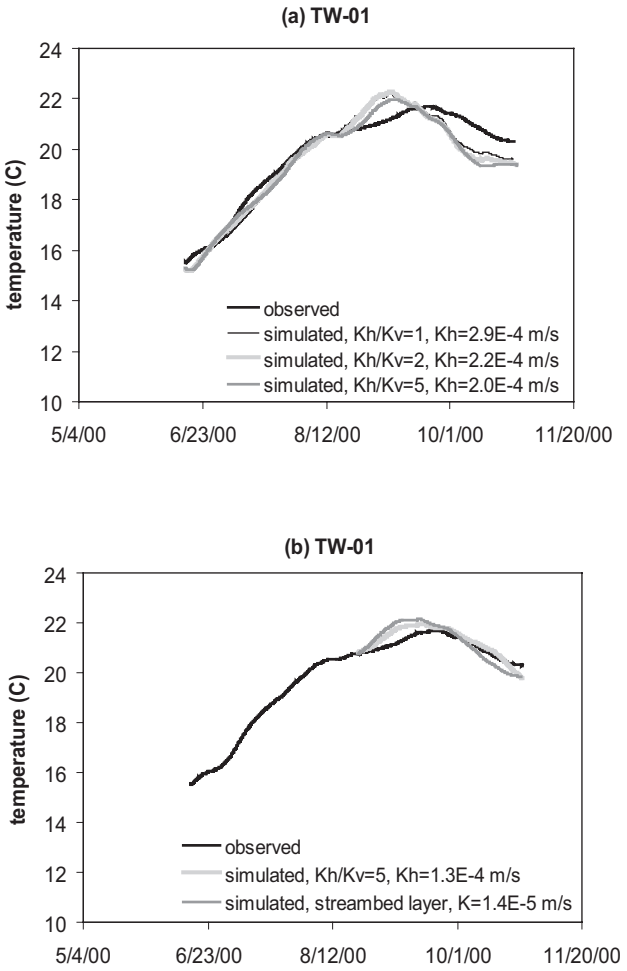

Figure 8. Best-fit simulated temperature profiles for different anisotropy values for well TW-01 (a) before August and (b) after August.

logs for wells TW-01, TW-13, and KSG-OW-01 indicated that the soil in the vicinity of these wells was predominantly sandy gravel. The estimated conductivities from these wells were the same order of magnitude. The soil near well TW-08 was mostly silty clay and sandy clay, and the estimated conductivity from this well was more than an order of magnitude smaller than the conductivities from wells TW-01, TW-13, and KSG-OW-01.

Hydraulic conductivities estimated from pumping tests ranged between 2.5×10^{-3} m/s to 6.5×10^{-3} m/s. For these tests, water was pumped from the collector wells and the subsequent drawdowns were measured at the monitoring wells. The conductivities estimated using the temperature method were about an order of magnitude less than these values. The temperature method estimated the hydraulic conductivity from the river to the observation well, while the pumping test estimated the conductivity from the pumping well to the monitoring well. Therefore, the low conductivity layer along the streambed was not incorporated in the estimates from the pumping tests, which resulted in larger conductivity estimates.

Horizontal fluxes calculated for each well using the best fit K value when $K_h/K_v = 5$ and the hydraulic gradient (Table 1) are also summarized in Table 3. The two lowest fluxes occur in wells TW-08 and KSG-OW-01, which have a nearly constant temperature profile (Figure 4) due to the lack of advective heat transport. The four remaining wells had much higher fluxes compared to wells TW-08 and KSG-OW-01, and they had distinct seasonal temperature profiles because of the increase in advective heat transport.

The root mean square error (RMSE) was used to quantify the goodness-of-fit between the simulated and observed results at the different anisotropies, and these values are summarized in Table 3 (a smaller RMSE value indicates a better fit). For well TW-01, $K_h/K_v = 2$ and 5 gives better fits to the data than $K_h/K_v = 1$ before mid-August. For well TW-13, $K_h/K_v = 5$ gives a better fit than $K_h/K_v = 1$ and 2. The RMSE for wells MW-93-14 and MW-93-18 decreases significantly as the anisotropy increases. Based on these results, an anisotropy of 5 generally gives the best match to the observed temperatures.

Two-Dimensional Temperature Distributions

Two-dimensional temperature distributions from the simulations are presented in Figure 11 for wells TW-13 and MW-93-18. Heat is transported both vertically and horizontally below the streambed; away from the streambed, heat is transported horizontally toward the observation well.

Figure 11 shows the effect of anisotropy on the temperature distribution when the hydraulic conductivity

Table 3
Summary of Temperature-Based Hydraulic Conductivities

Well	Best-Fit K_h (m/s) $K_h/K_v = 1$	RMSE	Best-Fit K_h (m/s) $K_h/K_v = 2$	RMSE	Best-Fit K_h (m/s) $K_h/K_v = 5$	RMSE	Horizontal Flux (m/s) = $K_h \times i$ Best Fit K_h, $K_h/K_v = 5$
TW-01	2.9E-04	0.28	2.2E-04	0.24	2.0E-04[a]	0.24	2.0E-05[a]
					1.3E-04[b]	0.32	1.3E-05[b]
TW-08	< 2.0E-05		< 2.1E-05		< 2.1E-05		< 7.8E-07
TW-13	6.9E-04	0.64	4.9E-04	0.50	4.1E-04	0.31	1.1E-05
MW-93-14	1.4E-04	0.65	1.4E-04	0.32	1.9E-04[a]	0.21	1.9E-05[a]
					1.2E-04[b]	0.17	1.2E-05[b]
MW-93-18	3.5E-05	1.18	4.1E-05	0.84	5.5E-05	0.56	1.2E-05
KSG-OW-01	< 4.6E-04		< 3.5E-04		< 2.9E-04		< 4.9E-06

[a] K_h before August 15, 2000
[b] K_h after August 15, 2000

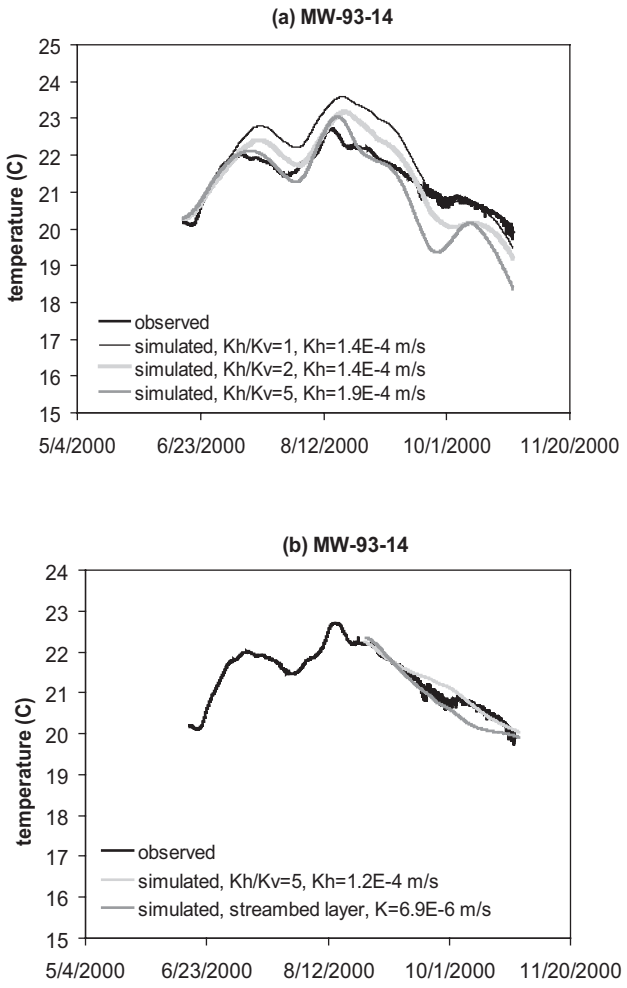

Figure 9. Best-fit simulated temperature profiles for different anisotropy values for well MW-93-14 (a) before mid-August and (b) after mid-August.

remains constant. This figure can be used to explain why the best fit *K* value decreases with increasing anisotropy in wells TW-01 and TW-13, but increases with increasing anisotropy in wells MW-93-14 and MW-93-18. The reason for this discrepancy is due to the proximity of the wells to the streambed. In wells TW-01 and TW-13, which are located away from the streambed, horizontal heat transport near these wells is greater over the same time period as the anisotropy increases (Figure 11, top row). Therefore, a smaller *K* is needed to obtain a good fit. In wells MW-93-14 and MW-93-18, which are located close to the streambed, the vertical flux near the wells becomes small enough as the anisotropy increases such that the amount of heat absorbed in the sediment results in lowering the ground water temperatures (Figure 11, bottom row). As a result, the temperatures at the wells are lower as the anisotropy increases and a larger *K* is needed to obtain a good fit.

Sensitivity Analyses

Sensitivity analyses were performed to investigate how ground surface temperatures, streambed layering, river stage level, and ground water level affected the simulated temperature profiles.

Ground Surface Temperatures

The unsaturated zone was included in our simulations since the ground surface temperatures could have impacted the ground water temperatures. Simulations conducted with and without the ground surface temperatures demonstrated that the surface temperatures did not affect the ground water temperatures. Therefore, a saturated flow model could be used for similar conditions as those in this example study site (i.e., a perennial stream and no precipitation). The unsaturated zone will play an important role when, for instance, the stream is ephemeral and there is precipitation.

Layering Below the Streambed

The change in the temperature profiles after August in wells TW-01 and MW-93-14 was further investigated by conducting simulations that included a thin layer of lower conductivity material below the streambed to represent the accumulation of fine-grained sediments and organic matter. We assumed this lower conductivity layer was uniform across the entire cross section of the streambed. The thickness of this layer was assumed to be 1 m at both locations.

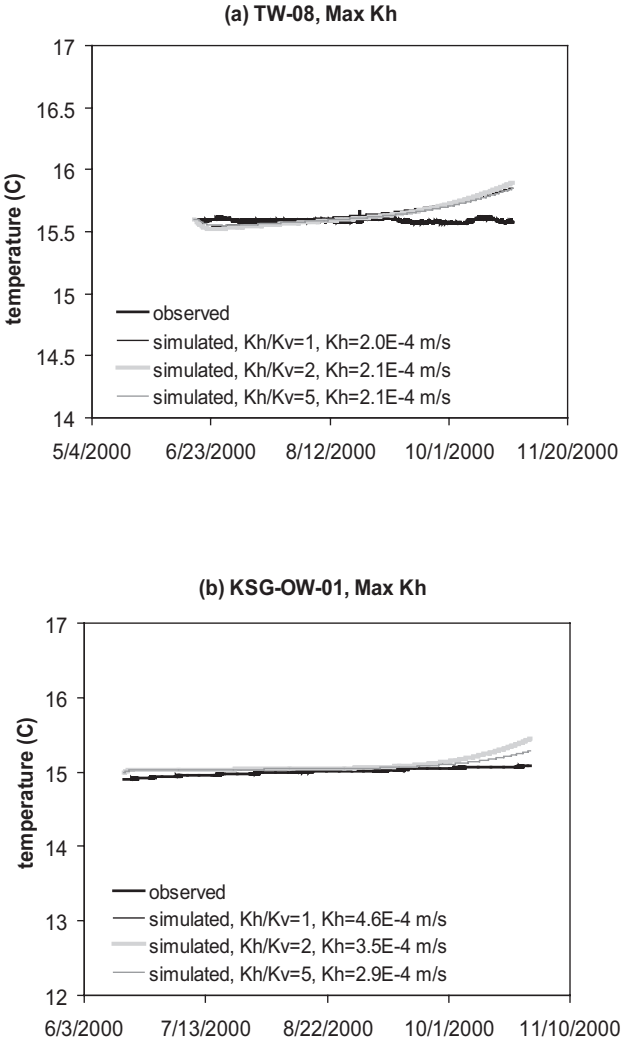

Figure 10. Maximum K_h values for different anisotropy values for wells (a) TW-08 and (b) KSG-OW-01.

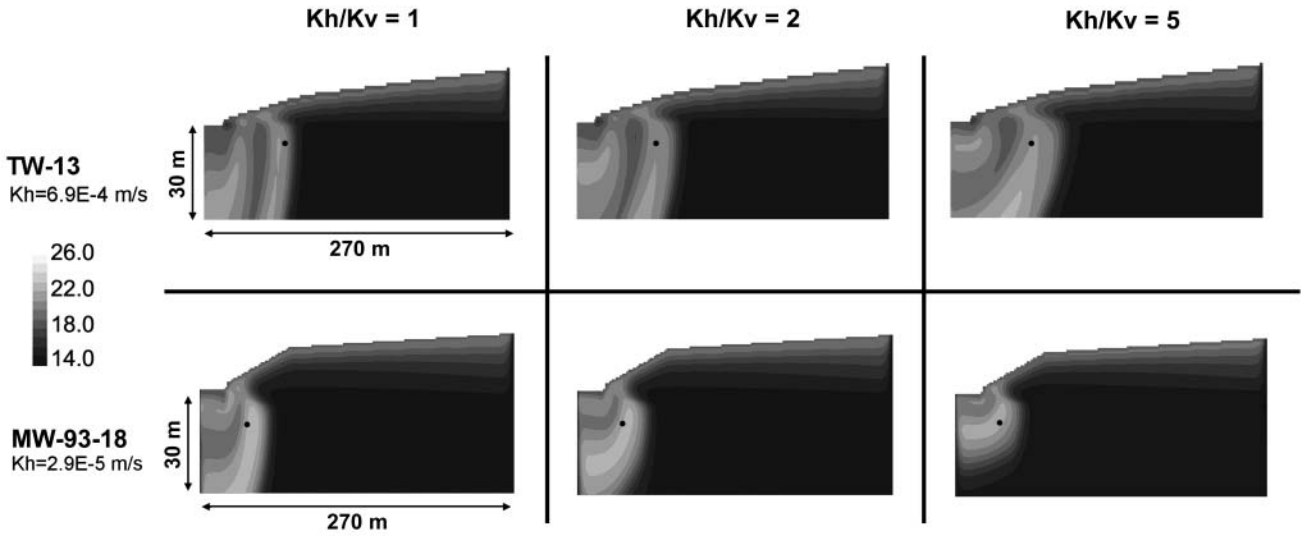

Figure 11. Two-dimensional temperature distribution after 100 d at different anisotropy values for wells TW-13 (top row) and MW-93-18 (bottom row).

The grid spacing in this layer was 1.5 m wide by 0.25 m deep. The simulated temperatures were fitted to the measured temperatures after August by varying the conductivity of the thin streambed layer. The hydraulic conductivity in the remainder of the simulation domain was set constant to the best fit value obtained during June/July when K_h/K_v = 5. The estimated conductivities of the streambed layer after August were 1.4×10^{-5} m/s for TW-01 and 6.9×10^{-6} m/s for MW-93-14 (Figures 8 and 9). Since flow was predominantly vertical below the streambed, estimates for the streambed conductivities during June/July were obtained from the best fit K_v values for these months when K_h/K_v = 5. These conductivities were 4.0×10^{-5} m/s for TW-01 and 3.8×10^{-5} m/s for MW-93-14. The reduction in streambed conductivity for TW-01 was > 60% after August and was > 80% for MW-93-14. Field data were not available to quantify the reduction in K or to indicate how thick and continuous the lower permeability streambed layer was. However, streambed sediment samples collected between June and September 2003 showed an increase in fine-grained deposits (Gorman 2004).

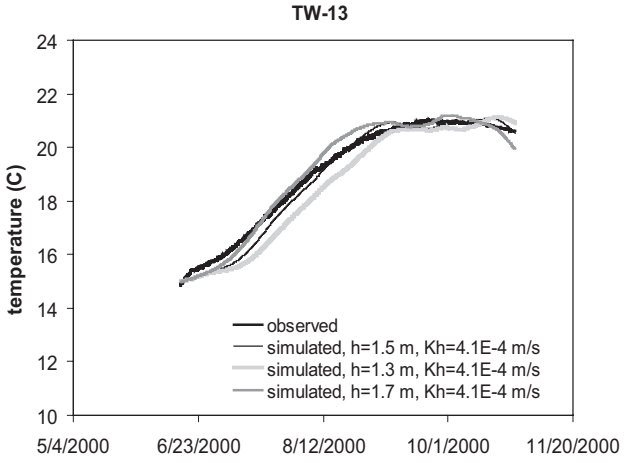

Figure 12. Sensitivity of simulated temperature profiles to the river stage in well TW-13.

River Stage Level

Our simulations assumed a constant river stage due to the control at the dam; however, small changes in the river stage may have occurred during the time period analyzed as a result of transient conditions due to anthropogenic conditions such as dam release and treatment plant release. The sensitivity of the simulated temperature profile to changes in river stage level was examined in well TW-13. The observed river stage level at this location was 1.5 m. The simulated temperature profiles using stage levels of 1.3 and 1.7 m and a hydraulic conductivity of 4.1×10^{-4} m/s are shown in Figure 12. The simulated temperature profile is shifted slightly left when the stage is 1.7 m compared to 1.5 m because the higher river stage level enhances the flow velocity and advective heat transport. When the stage is 1.3 m, the simulated profile is shifted slightly right because the flow velocity decreases and the advective heat transport is reduced compared to the results for a stage of 1.5 m. In Figure 12, changes in the simulated temperature profiles at the different stage levels are noticeable after about one month. Small changes in stage level in the study area most likely occurred over much shorter time periods (i.e., days) because the dam was raised. Therefore, the stage changes during the study period should have a relatively minor effect on the simulated temperature profiles.

In wells TW-01 and MW-93-14, we attributed the change in the temperature profile after August to a decrease in hydraulic conductivity. A large decrease in stage would be required to induce a change in the temperature profile of this magnitude. Specifically, a decrease in the stage to 1.0 and 0.7 m for wells TW-01 and MW-93-14, respectively, was necessary to obtain a better fit to the observed data after August if we assumed the effective hydraulic conductivity remained constant. A decrease in river stage of 0.5 m or more did not occur during the summer and fall months since the maximum measured decrease in stage further upstream of the study area was only ~0.2 m.

Ground Water Level

The sensitivity of the simulated temperature profiles to the ground water level was examined by running simulations using only the average water level. As an example, the simulated temperature profile using the average water level in MW-93-18 is shown in Figure 7 for $K_h = 5.5 \times 10^{-5}$ m/s and $K_h/K_v = 5$. The water level in well MW-93-18 varies substantially (up to 2.5 m) over the study period since it is close to the pumping wells. The simulated temperature profile using the average water level differs only slightly from the result using the variable water level. This result demonstrates that the simulated temperature profiles are not very sensitive to the changes in water level, even when the well is in the vicinity of pumping wells.

Summary and Conclusions

Seasonal ground water temperature profiles and water levels were used to estimate alluvial aquifer hydraulic conductivities at our example study site, the Russian River in Sonoma County, California. The seasonal ground water temperatures in the six wells analyzed along this site varied by < 0.2°C in two wells to nearly 8°C in the other four wells. The range in observed temperature fluctuations was primarily attributed to the proximity of the wells to pumping facilities. Based on these temperature variations, the estimated conductivities varied up to two orders of magnitude over these six locations. The simulated temperature profiles generally fit the observed ones best when an anisotropy of 5 was used.

In some locations, a change in the observed temperature profile occurred through the summer and fall, most likely due to deposition of fine-grained sediment and organic matter plugging the streambed. A reasonable fit to this change in temperature profile was obtained by decreasing the effective hydraulic conductivity in the simulations. Other factors such as changes in the ground water level and river stage were demonstrated not to be the cause of the change in the temperature profile. Simulations were also conducted where a thin low conductivity layer was placed below the streambed to represent the plugging that had occurred; a reasonable fit to the change in the observed temperature profiles was also obtained. The most significant decrease in conductivity occurred in the region closest to the dam. This finding indicated that temperature patterns during the winter and spring months should also be analyzed to examine the annual variation in hydraulic conductivity, particularly the change in conductivity after the dam has been lowered and the streambed has been flushed during the winter months. The temporal and spatial variations in hydraulic conductivities obtained in this study will be incorporated into a regionwide model currently under development.

One limitation of the approach used in this study was that the simulations were conducted in two dimensions. Three-dimensional effects due to pumping were not included. Even though a two-dimensional model was used in this study, reasonable matches of the simulated temperature profiles with the observed profiles were obtained. Another limitation was that information from only one well was used for each cross section. For observation wells located away from the pumping wells, water level information from one location did not provide enough information to demonstrate that the two-dimensional cross section was actually along a flow line. In addition, the assumption that the flow beneath the river was symmetric cannot be verified using information from only one well. Water level and temperature data on the other side of the stream should also be used in the simulations if available. Heterogeneities along the streambed and in the aquifer can also play an important role on ground water flow (Woessner 2000), but these effects were not captured with the homogenous sand layer used in this study. Additional field data are needed to better characterize the heterogeneity in this study area.

The simulated temperature profiles were much more sensitive to changes in K compared to changes in the river stage and well water level. Therefore, even with limited data on river stage and well water levels or errors in these measurements, estimates of K can still be obtained using the method described in this paper. This paper demonstrates that seasonal ground water temperatures monitored in observation wells, used in conjunction with water levels, provide an effective means of estimating alluvial aquifer hydraulic conductivities. This method should have wide application to stream-aquifer systems where seasonal ground water temperature variations occur.

Acknowledgments

The authors would like to thank R. Niswonger , C.-F. Tsang, G. Pohll, M.P. Anderson, and two anonymous reviewers for helpful comments and suggestions on this paper. This work was supported by SCWA, through U.S. Department of Energy Contract No. DE-AC03–76SF00098.

Editor's Note: The use of brand names in peer-reviewed papers is for identification purposes only and does not constitute endorsement by the authors, their employers, or the National Ground Water Association.

References

Bartolino, J.R., and R.G. Niswonger. 1999. Numerical simulation of vertical ground-water flux of the Rio Grande from ground-water temperature profiles, central New Mexico. U.S. Geological Survey Water-Resources Investigations Report 99–4212.

Boyle, J.M., and Z.A. Saleem. 1979. Determination of recharge rates using temperature-depth profiles in wells. *Water Resources Research* 15, no. 6: 1616–1622.

Bravo, H.R., J. Feng, and R.J. Hunt. 2002. Using groundwater temperature data to constrain parameter estimation in a groundwater flow model of a wetland system. *Water Resources Research* 38, no. 8: 10.1029/2000WR000172: 28–1–28–14.

California Department of Water Resources. 1983. Evaluation of ground water resources: Sonoma County, Volume 5: Alexander Valley and Healdsburg area. California Department of Water Resources Bulletin 118–4.

Constantz, J., and C.L. Thomas. 1996. The use of streambed temperature profiles to estimate the depth, duration, and rate of percolation beneath arroyos. *Water Resources Research* 32, no. 12: 3597–3602.

Constantz, J., D. Stonestrom, A.E. Stewart, R. Niswonger, and T.R. Smith. 2001. Analysis of streambed temperatures in ephemeral channels to determine streamflow frequency and duration. *Water Resources Research* 37, no. 2: 317–328.

Constantz, J., A.E. Stewart, R. Niswonger, and L. Sarma. 2002. Analysis of temperature profiles for investigating stream losses beneath ephemeral channels. *Water Resources Research* 38, no. 12: 1316, doi:10.1029/2001WR001221.

Constantz, J., M.H. Cox, and G.W. Su. 2003. Comparison of heat and bromide as ground water tracers near streams. *Ground Water* 41, no. 5: 647–656.

de Marsily, G. 1986. *Quantitative Hydrogeology: Groundwater Hydrology for Engineers*. San Diego, California: Academic Press.

Ferguson, G., A.D. Woodbury, and G.L.D. Matile. 2003. Estimating deep recharge rates beneath an interlobate moraine using temperature logs. *Ground Water* 41, no. 5: 640–646.

Gorman, P. 2004. Spatial and temporal variability of hydraulic properties in the Russian River streambed, Central Sonoma County, California. M.S. thesis, San Francisco State University.

Healy, R.W., and A.D. Ronan. 1996. Documentation of computer program VS2DH for simulation of energy transport in variably saturated porous media. U.S. Geological Survey Water-Resources Investigations Report 96–4230.

Hsieh, P.A., W. Wingle, and R.W. Healy. 2000. VS2DI—A graphical software package for simulating fluid flow and solute or energy transport in variably saturated porous media. U.S. Geological Survey Water-Resources Investigations Report 99–4130.

Hunt, R.J., D.P. Krabbenhoft, and M.P. Anderson. 1996. Groundwater inflow measurements in wetland systems. *Water Resources Research* 32, no. 3: 495–508.

Kipp, K.L. 1987. HST3D: A computer code for simulation of heat and solute transport in three-dimensional ground water systems. U.S. Geological Survey Water-Resources Investigations Report 86–4095.

Lapham, W.W. 1989. Use of temperature profiles beneath streams to determine rates of vertical ground water flow and vertical hydraulic conductivity. U.S. Geological Survey Water Supply Paper 2337.

Mihevc, T., G. Pohll, R. Niswonger, and E. Stevick. 2001. Truckee canal seepage analysis in the Fernley/Wadsworth area. Desert Research Institute Publication No. 41176.

Ronan, A.D., D.E. Prudic, C.E. Thodal, and J. Constantz. 1998. Field study and simulation of diurnal temperature effects on infiltration and variably saturated flow beneath an ephemeral stream. *Water Resources Research* 34, no. 9: 2137–2153.

Silliman, S.E., and D.F. Booth. 1993. Analysis of time-series measurements of sediment temperature for identification of gaining vs. losing portions of Judy Creek, Indiana. *Journal of Hydrology* 146, no. 1: 131–148.

Stonestrom, D.A., and J. Constantz. 2003. Heat as a tool for studying the movement of ground water near streams. U.S. Geological Survey Circular 1260.

Taniguchi, M. 1993. Evaluation of vertical groundwater fluxes and thermal properties of aquifers based on transient temperature-depth profiles. *Water Resources Research* 29, no. 7: 2021–2026.

Taniguchi, M., J. Shimada, T. Tanaka, I. Kayane, Y. Sakura, Y. Shimano, S. Dapaah-Siakwan, and S. Kawashima. 1999. Disturbances of temperature depth profiles due to surface climate change and subsurface water flows, 1. An effect of linear increase in surface temperature caused by global warming and urbanization in the Tokyo metropolitan area, Japan. *Water Resources Research* 35, no. 5: 1507–1517.

Woessner, W.W. 2000. Stream and fluvial plan ground water interactions: Rescaling hydrogeologic thought. *Ground Water* 38, no. 3: 423–429.

Woodbury, A.D., and L. Smith. 1988. Simultaneous inversion of hydrogeologic and thermal data, 2. Incorporation of thermal data. *Water Resources Research* 24, no. 3: 356–372.